Viscoacoustic modeling and imaging using low-rank approximation[a]

[a]Published in Geophysics, 80, A103-A108, (2015)

Junzhe Sun[*1], *Tieyuan Zhu*[1], *and Sergey Fomel*[1]

ABSTRACT

A constant-Q wave equation involving fractional Laplacians was recently introduced for viscoacoustic modeling and imaging. This fractional wave equation has a convenient mixed-domain space-wavenumber formulation, which involves the fractional-Laplacian operators with a spatially varying power. We propose to apply low-rank approximation to the mixed-domain symbol, which enables a space-variable attenuation specified by the variable fractional power of the Laplacians. Using the proposed approximation scheme, we formulate the framework of the Q-compensated reverse-time migration (Q-RTM) for attenuation compensation. Numerical examples using synthetic data demonstrate the improved accuracy of using low-rank wave extrapolation with a constant-Q fractional-Laplacian wave equation for seismic modeling and migration in attenuating media. Low-rank Q-RTM applied to viscoacoustic data is capable of producing images comparable in quality with those produced by conventional RTM from acoustic data.

INTRODUCTION

Modeling seismic wave propagation in attenuating media accounts for the effective anelastic characteristics of the real Earth (Carcione, 2007). Numerous studies have shown that many of the hydrocarbon prospecting areas, such as those where gas accumulations are present, strongly attenuate seismic waves (Dvorkin and Mavko, 2006). Seismic attenuation can be expressed as a combined effect of energy loss and velocity dispersion.

Attenuation effects can be modeled by incorporating the quality factor, Q, in the time-domain wave equation. One of the classic approaches involves a superposition of mechanical elements (e.g., Maxwell and standard linear solid elements) to characterize Q, and is known as approximate constant-Q models (Liu et al., 1976; Blanch et al., 1995; Carcione, 2007; Zhu et al., 2013). The approximate constant-Q approach suffers from large computational and memory requirements. Kjartansson (1979) initially proposed a constant-Q model that assumes a linear relationship between the attenuation coefficient and frequency. This model was proven accurate in capturing a nearly constant Q behavior within the seismic frequency band. However, early implementations

of the constant-Q model involved a fractional time derivative, which required storing the whole history of the wavefield (Caputo and Mainardi, 1971). This requirement rendered the memory cost too high for practical applications, even when the fractional operator was truncated after a certain time period (Podlubny, 1999; Carcione et al., 2002; Carcione, 2009). To overcome this issue, fractional-Laplacian operators (Chen and Holm, 2004) have been introduced to approximate the constant-Q viscoacoustic wave equation (Carcione, 2010; Zhu and Harris, 2014). The fractional-Laplacian approach is attractive because it can be conveniently formulated in the wavenumber domain using Fourier transforms and without introducing any extra equations or variables (Carcione, 2010). Using this approach, Zhu and Harris (2014) developed a decoupled wave equation that accounts separately for amplitude attenuation and phase dispersion effects, thus allowing for correct compensation for both factors during back propagation by reversing the sign of the attenuation operator and keeping the sign of the dispersion operator unchanged (Zhu, 2014).

Zhu et al. (2014) further proposed to use the fractional-Laplacian Q-compensated wave equation for reverse-time migration. Zhang et al. (2010) applied an analogous approach derived from normalization transforms. Alternative strategies for compensating for attenuation in seismic migration include methods based on one-way wave-equation migration (WEM) and its dispersion relation (Valenciano and Chemingui, 2012), as well as methods based on Kirchhoff migration and reverse-time migration (RTM), with time-variant Q filters (Cavalca et al., 2013). Dutta and Schuster (2014) used least-squares RTM for attenuation compensation based on standard linear solid (SLS) model and its adjoint operator (Blanch and Symes, 1995), with a simplified stress-strain relation, which incorporated a single relaxation mechanism (Robertsson et al., 1994; Blanch et al., 1995).

The fractional-Laplacian approach was previously implemented using either a pseudo-spectral method, by averaging the fractional power of the Laplacian operator as an approximation (Zhu and Harris, 2014), or a finite-difference approach (Lin et al., 2009). In this paper, we propose to apply a low-rank approximation scheme (Fomel et al., 2013; Sun and Fomel, 2013) to implement decoupled fractional Laplacians of Zhu and Harris (2014) in wave extrapolation, with the goal of accurately capturing spatially-varying fractional power. The advantage of the low-rank approach is its ability to directly approximate the mixed-domain wave extrapolation operator with a separable representation, which minimizes the number of fast Fourier transforms (FFTs) per time step. Additionally, we derive the adjoint of the forward modeling operator, which correctly compensates for velocity dispersion but not amplitude loss. The proposed operator and its adjoint can be used in least-squares RTM to recover the true reflectivity of the attenuating medium through iterations of migration and modeling (Sun et al., 2014). In this paper, we implement Q-RTM using an operator that compensates for amplitude loss during back propagation of the viscoacoustic data (Zhu et al., 2014). When used with the cross-correlation imaging condition, the attenuation-compensated operator is capable of producing images with improved illumination in the attenuating zone. We apply the low-rank Q-RTM to synthetic data generated from a constant-Q model to demonstrate the effectiveness of attenuating

compensation by the proposed method.

THEORY

A constant-Q model assumes that the attenuation coefficient is linear in frequency (Kjartansson, 1979). The time-domain viscoacoustic wave equation for constant-Q model can be written as (Carcione et al., 2002)

$$\frac{\partial^{2-2\gamma} P}{\partial t^{2-2\gamma}} = c^2 \omega_0^{-2\gamma} \nabla^2 P \;, \tag{1}$$

where $\mathbf{x}$ is the spatial coordinate vector, $P(\mathbf{x}, t)$ is the pressure wavefield,

$$\gamma(\mathbf{x}) = \arctan(1/Q(\mathbf{x}))/\pi \tag{2}$$

is a dimensionless parameter, ∇^2 is the Laplacian operator,

$$c^2(\mathbf{x}) = c_0^2(\mathbf{x}) \cos^2(\pi\gamma(\mathbf{x})/2) \;, \tag{3}$$

and $c_0(\mathbf{x})$ is the velocity model defined at the reference frequency ω_0. When Q is finite, γ is greater than zero, and the wave equation involves a fractional time derivative.

In a homogeneous medium, considering the plane-wave solution $e^{(i\omega t - i\tilde{\mathbf{k}}\cdot\mathbf{x})}$, where ω is the angular frequency and $\tilde{\mathbf{k}}$ is the complex wavenumber vector and substituting it into equation 1, leads to the dispersion relation

$$\frac{\omega^2}{c^2} = (i)^{2\gamma} \omega_0^{-2\gamma} \omega^{2\gamma} \tilde{\mathbf{k}}^2 \;. \tag{4}$$

Starting from equation 4, Zhu and Harris (2014) derived the following approximate dispersion relation:

$$\frac{\omega^2}{c^2} = -\eta |\mathbf{k}|^{2\gamma+2} - i\omega\tau |\mathbf{k}|^{2\gamma+1} \;, \tag{5}$$

which corresponds to the following constant-Q wave equation with fractional Laplacians:

$$\frac{1}{c^2}\frac{\partial^2 P}{\partial t^2} = \nabla^2 P + \{\eta(-\nabla^2)^{\gamma+1} - \nabla^2\} P + \tau \frac{\partial}{\partial t}(-\nabla^2)^{\gamma+1/2} P \;, \tag{6}$$

where $\eta = -c_0^{2\gamma}\omega_0^{-2\gamma}\cos(\pi\gamma)$ and $\tau = -c_0^{2\gamma-1}\omega_0^{-2\gamma}\sin(\pi\gamma)$. Note that both c_0 (the phase velocity) and γ (the fractional power) can be heterogeneous (depending on $\mathbf{x}$). Solving for ω in equation 5 yields:

$$\omega = \frac{-ip_1 + p_2}{2} \;, \tag{7}$$

where:

$$p_1 = \tau c^2 |\mathbf{k}|^{2\gamma+1} \;, \tag{8}$$

$$p_2 = \sqrt{-\tau^2 c^4 |\mathbf{k}|^{4\gamma+2} - 4\eta c^2 |\mathbf{k}|^{2\gamma+2}} \;. \tag{9}$$

The phase function $\phi(\mathbf{x}, \mathbf{k}, \Delta t)$ that determines the phase shift of wavefield for propagation in time is then defined as

$$\phi_1(\mathbf{x}, \mathbf{k}, \Delta t) = \mathbf{k} \cdot \mathbf{x} + \frac{-ip_1 + p_2}{2} \Delta t \tag{10}$$

and can be supplied to the low-rank one-step wave extrapolation algorithm (Sun and Fomel, 2013).

To compensate for attenuation, reversing the sign of the second term on the right hand side of equation 5 can amplify the amplitude, while the other term must be kept unchanged to counteract the dispersion effects (Zhu, 2014). Thus, the attenuation-compensated constant-Q wave equation corresponds to the dispersion relation:

$$\frac{\omega^2}{c^2} = -\eta |\mathbf{k}|^{2\gamma+2} + i\omega\tau |\mathbf{k}|^{2\gamma+1} \ , \tag{11}$$

which defines the complex-conjugate phase function:

$$\phi_2(\mathbf{x}, \mathbf{k}, \Delta t) = \bar{\phi_1}(\mathbf{x}, \mathbf{k}, \Delta t) = \mathbf{k} \cdot \mathbf{x} + \frac{ip_1 + p_2}{2} \Delta t \ . \tag{12}$$

Both ϕ_1 and ϕ_2 involve the fractional power of wavenumber, and depend on both $\mathbf{x}$ and $\mathbf{k}$, the Fourier transform pair. The low-rank one-step wave extrapolation operator (Sun and Fomel, 2013) provides a convenient way to utilize the phase function to extrapolate a viscoacoustic wavefield, while allowing $\gamma(\mathbf{x})$, the fractional power coefficient, to vary in space. The one-step mixed-domain operator has the form of the following Fourier integral operator:

$$P(\mathbf{x}, t + \Delta t) = \int \hat{P}(\mathbf{k}, t)\, e^{i\,\phi(\mathbf{x},\mathbf{k},\Delta t)}\, d\mathbf{k} \ , \tag{13}$$

where $\hat{P}$ is the spatial Fourier transform of P. Its adjoint form can be expressed as

$$\hat{P}(\mathbf{k}, t) = \int P(\mathbf{x}, t + \Delta t)\, e^{-i\,\bar{\phi}(\mathbf{x},\mathbf{k},\Delta t)}\, d\mathbf{x} \ , \tag{14}$$

where $\bar{\phi}$ denotes the complex conjugate of ϕ. Substituting equation 10 into equation 13, we can write the forward extrapolation operator explicitly as

$$P(\mathbf{x}, t + \Delta t) = \int \hat{P}(\mathbf{k}, t)\, e^{i\,\phi_1(\mathbf{x},\mathbf{k},\Delta t)}\, d\mathbf{k} = \int \hat{P}(\mathbf{k}, t)\, e^{i\mathbf{k}\cdot\mathbf{x} + (p_1 + ip_2)\,\Delta t/2}\, d\mathbf{k} \ . \tag{15}$$

The corresponding adjoint operator takes the form:

$$\hat{P}_{adj}(\mathbf{k}, t) = \int P(\mathbf{x}, t + \Delta t)\, e^{-i\,\bar{\phi_1}(\mathbf{x},\mathbf{k},\Delta t)}\, d\mathbf{x} = \int P(\mathbf{x}, t + \Delta t)\, e^{-i\mathbf{k}\cdot\mathbf{x} + (p_1 - ip_2)\,\Delta t/2}\, d\mathbf{x} \ . \tag{16}$$

To make the computation feasible, we apply low-rank decomposition proposed by Fomel et al. (2013) to approximate the wave extrapolation symbol in equations 15 and 16.

Note that the adjoint operator compensates for velocity dispersion. Because the sign of p_1 remains unchanged, the amplitude of waves will be attenuated during backward propagation using equation 16. This means that the adjoint operator may not be well suited for RTM because the backward wavefield would be attenuated twice. However, the adjoint operator can be supplied into the framework of least-squares RTM which can then iteratively recover the amplitude loss caused by viscoacoustic attenuation (Sun et al., 2014).

An alternative strategy for backward wave propagation is to try compensating for the full attenuation effect (both amplitude loss and velocity dispersion) using the operator

$$P_{comp}(\mathbf{x}, t+\Delta t) = \int \hat{P}(\mathbf{k}, t)\, e^{i\,\phi_2(\mathbf{x},\mathbf{k},\Delta t)}\, d\mathbf{k} = \int \hat{P}(\mathbf{k}, t)\, e^{i\mathbf{k}\cdot\mathbf{x}+(-p_1+ip_2)\,\Delta t/2}\, d\mathbf{k}\ , \quad (17)$$

which is the adjoint of

$$\hat{P}_{comp}(\mathbf{k}, t) = \int P(\mathbf{x}, t+\Delta t)\, e^{-i\,\bar{\phi}_2(\mathbf{x},\mathbf{k},\Delta t)}\, d\mathbf{x} = \int P(\mathbf{x}, t+\Delta t)\, e^{-i\mathbf{k}\cdot\mathbf{x}+(-p_1-ip_2)\,\Delta t/2}\, d\mathbf{x}\ . \quad (18)$$

In application to RTM, operator in equation 17 has an exponentially growing term which can amplify the energy in the forward-propagated source wavefield. In the same manner, operator in equation 18 can compensate for the amplitude loss in the backward-propagated receiver wavefield. In order to avoid magnifying high-frequency components during wave propagation, we employ a low-pass Tukey filter for the attenuation and dispersion operators in the wavenumber domain (Zhu et al., 2014). A complex-valued imaging condition that compensates for both velocity dispersion and amplitude loss can be obtained by cross-correlating the source and receiver wavefields modeled by equations 17 and 18 (Zhu et al., 2014).

In this way, the migrated viscoacoustic data gets corrected for attenuation due to viscoacoustic material encountered along the wave path. As will be demonstrated in the numerical examples, Q-compensated RTM is capable of enhancing illumination in areas where attenuating material is present. For a more accurate compensation of attenuation, operators 17 and 18 can be used to design a preconditioner in iterative least-squares RTM.

NUMERICAL EXAMPLES

Two-layer model

The purpose of our first example is to investigate the accuracy of the solution of the constant-Q wave equation using the proposed low-rank scheme, in the presence of a sharp contrast in both velocity and Q. We use an isotropic two-layer model with $v = 1800\ m/s$ in the top layer and $v = 3600\ m/s$ in the bottom layer. The model is discretized on a 200×200 grid, with a spatial sampling of $8\ m$ along both

X and Z directions. An explosive source with a peak frequency of 50 Hz is located at the center. The reference frequency is $\omega_0 = 1500\ Hz$. Wavefield snapshots are taken at $t = 330\ ms$. Figure 1a shows the acoustic case, in which the model has the velocity discontinuity but no attenuation ($Q = \infty$). For comparison, Figure 1b demonstrates the effect of homogeneous attenuation where $Q = 30$. Both velocity dispersion and amplitude loss can be observed. In Figure 1c, we set $Q = 30$ in the top layer and $Q = 100$ in the bottom layer. The transmitted arrival exhibits less attenuation compared with that in Figure 1b. In Figure 1d, both velocity and Q remain the same as those in Figure 1c; however, the fractional power of Laplacians, γ, is taken to be the averaged value, which corresponds to the original implementation by Zhu and Harris (2014). To compare the results modeled by the two strategies, a middle trace at $x = 800\ m$ is extracted from both wavefield snapshots (Figures 1c and 1d). Figure 2 shows the two traces, along with their difference. Errors caused by using a constant γ instead of a spatially varying γ can be easily observed.

Marmousi Q model

In the second example, we use a synthetic attenuation model to investigate the effect of Q compensation in RTM. Figure 3a shows the Marmousi velocity model. We build a corresponding Q model (Figure 3b) on the same grid. The model features three highly attenuative zones in the shallow parts of the model. This kind of an attenuation patter can be caused in reality by the presence of a gas accumulation. The model is discretized on a 241×961 grid with a spacing of 12.5 m in both horizontal and vertical directions. A total of 64 shots with a horizontal spacing of 187.5 m were used, starting from 25 m, and the source is a Ricker wavelet with a peak frequency of 20 Hz. Receivers have a spacing of 12.5 m, starting from 0 m and ending at 12000 m. For simplicity of modeling, both sources and receivers are located at $-62.5\ m$ depth. The data have a temporal sampling of 2 ms, with a total length of 8 s. First, acoustic modeling is used to generate acoustic data (Figure 4a), and then viscoacoustic modeling is used to generate viscoacoustic data (Figure 4b), accounting for seismic attenuation during wave propagation. We first apply acoustic RTM on the (non-attenuated) acoustic data to generate a reference image (Figure 5a). The image generated by non-compensated RTM using viscoacoustic data (Figure 5b) suffers from a lack of illumination within and below the attenuative region. Using the proposed Q-RTM according to equations 17 and 18 (Figure 5c), the amplitude of the parallel normal faults and anticline structures has been recovered to a large extent, and image resolution inside and below gas has been greatly enhanced. The Tukey filter is applied with a cutoff frequency of 100 Hz with a taper ratio of 0.4. We extract the trace at $X = 6875\ m$ and Z between 500 m and 3000 m from the three images, and use the acoustic RTM image from migrating acoustic data as a reference (shown in Figures 6a and 6b). The comparison shows that the conventional RTM applied to viscoacoustic data suffers from the effects of phase rotation and amplitude attenuation, especially in the deeper part of the image, while the Q-compensated image highly resembles the non-attenuated acoustic image in both amplitude and phase. To test the sensitivity

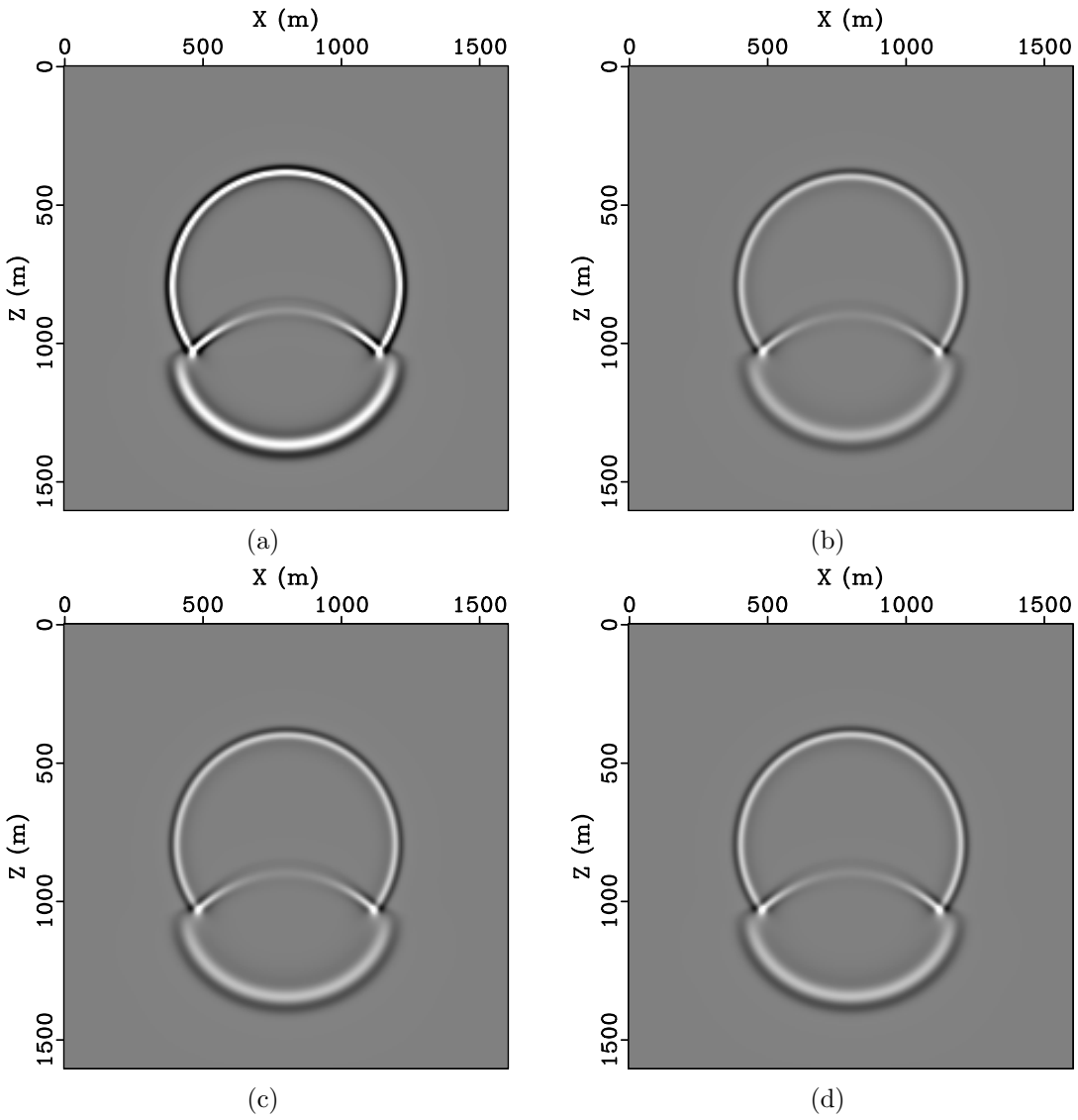

Figure 1: Viscoacoustic wave propagation in a two-layer model: (a) acoustic modeling with $v = 1800\ m/s$ in top layer and $v = 3600\ m/s$ in bottom layer; (b) same velocity as (a), homogeneous $Q = 30$; (c) same velocity as (a), $Q = 30$ in top layer and $Q = 100$ in bottom layer; (d) wavefield propagated using a constant averaged fractional power γ using same model as (c).

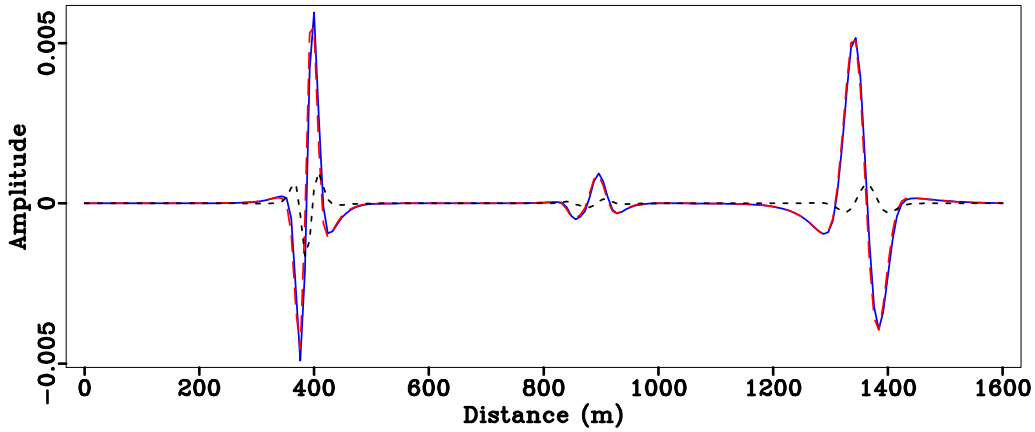

Figure 2: Traces at $x = 800\ m$ extracted from wavefield snapshots and their difference. Red, long-dashed line corresponds to averaged γ; blue, solid line corresponds to variable γ; black, shot-dashed line is their difference.

of the proposed method to noise in the data, we add Gaussian random noise to the viscoacoustic data with a signal-to-noise ratio (SNR) of 0.9 (Figure 4c). Applying Q-RTM to the noisy data leads to a slightly noisier image (Figure 6c). However, migration remains stable and all the reflectors remain well-imaged.

DISCUSSION

For both acoustic RTM and Q-RTM in the Marmousi example, with a time step size of 2 ms, we used the low-rank approximation with a rank of 4, corresponding to 5 complex-to-complex FFTs per time step (with one additional forward FFT). Therefore, both methods had the same computational cost. A pseudo-spectral method would require 4 real-to-complex FFTs per time step to calculate the two fractional Laplacians in the second-order wave equation (equation 6). On the other hand, the SLS model with L relaxation mechanisms would require to solve $3 + L$ equations in the $2D$ case or $4 + L$ equations in the $3D$ case (Zhu et al., 2013), and has an effective cost of 4 real-to-complex FFTs per time step when implemented using a pseudo-spectral method. However, a pseudo-spectral implementation poses a strict limit on time step size due to its finite-difference approximation of time derivatives, and thus may require a larger number of time steps to propagate the same length of time compared with the proposed method (Sun and Fomel, 2013).

CONCLUSIONS

We introduce a low-rank viscoacoustic wave extrapolation method based on the constant-Q wave equation with decoupled fractional Laplacians. The proposed numerical method can handle an arbitrarily variable fractional power of the wavenum-

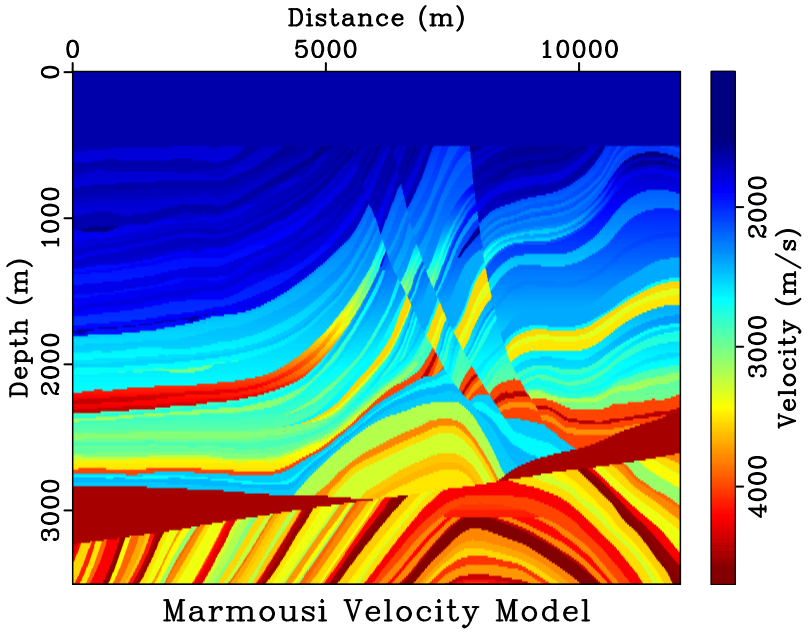

(a)

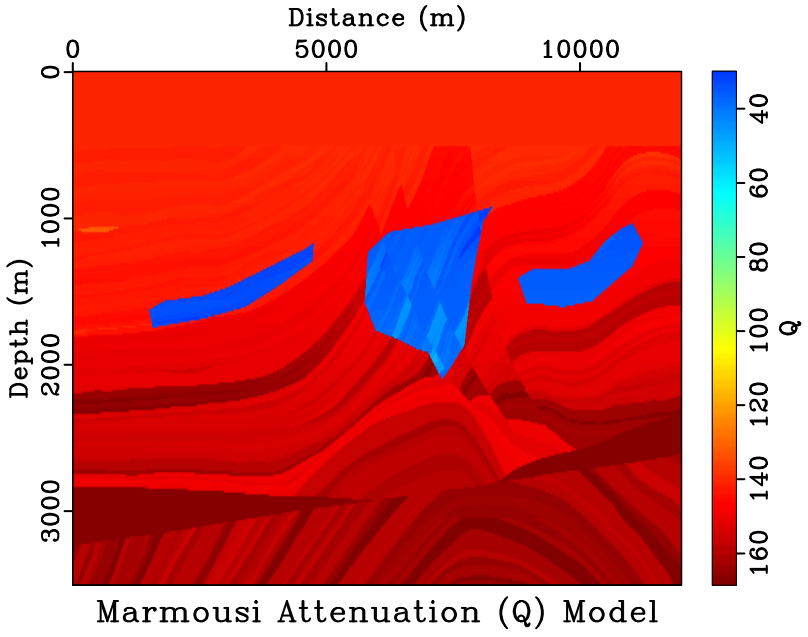

(b)

Figure 3: Marmousi velocity/attenuation (Q) model. (a) Marmousi velocity model; (b) Marmousi Q model.

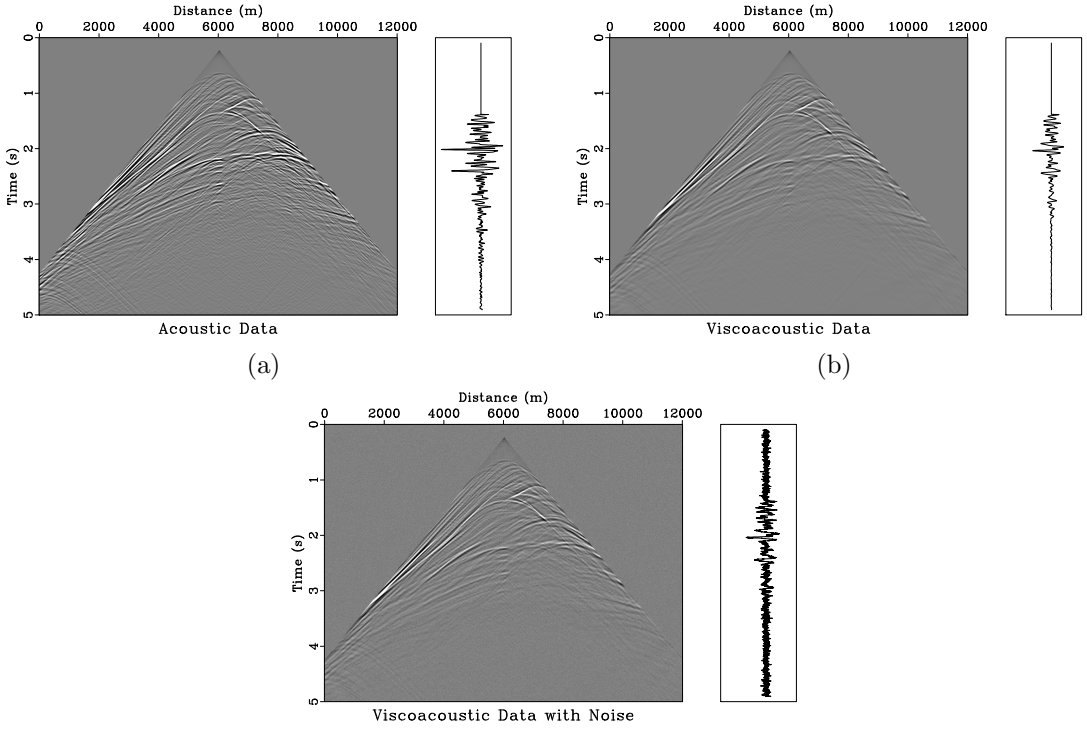

Figure 4: Common-shot gathers used for RTM and Q-RTM at $X = 6025\ m$. A total length of 8 s has been recorded, while only the first 5 s is displayed. (a) Acoustic data; (b) viscoacoustic data. (c) viscoacoustic data with added random noise (SNR = 0.8). The right panel shows a trace extracted from $X = 4375\ m$.

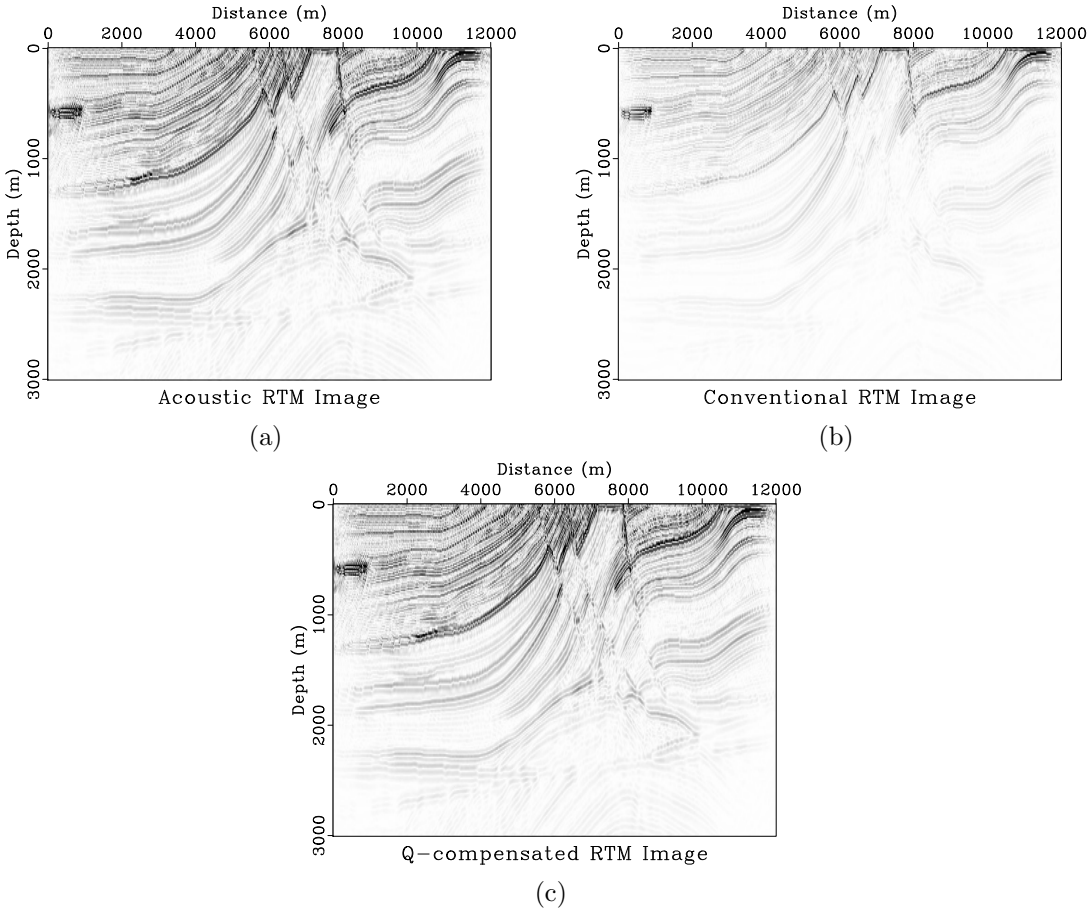

Figure 5: RTM images obtained using acoustic and visco-acoustic data. (a) Acoustic RTM image using acoustic data; (b) Acoustic RTM image using viscoacoustic data. (c) Q-RTM image using viscoacoustic data.

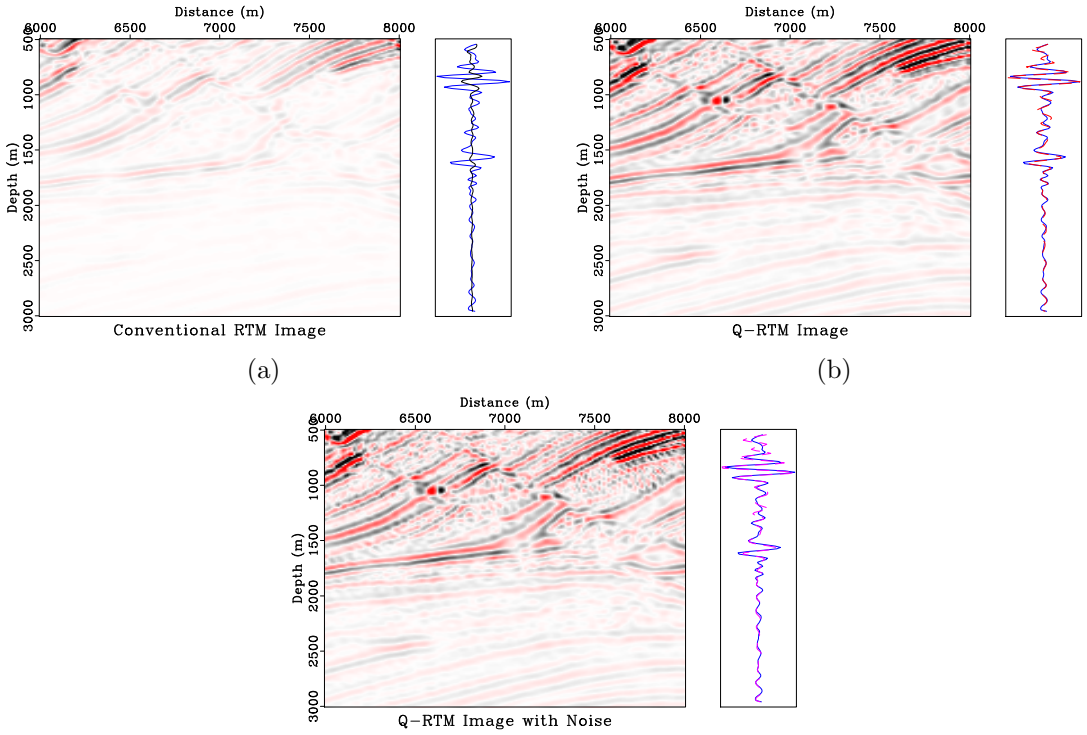

Figure 6: A portion of RTM images obtained using different approaches. (a) acoustic RTM image using viscoacoustic data; (b) Q-RTM image using viscoacoustic data; (c) Q-RTM image using viscoacoustic data with added noise. The right panel compares the trace at $X = 6875\ m$ from the corresponding image with the reference image obtained by applying acoustic RTM on acoustic data. Blue solid line refers to the reference image; black solid line refers to the non-compensated image; red dashed line refers to the compensated image; pink dashed line refers to the compensated image using noisy data.

ber, and thus is capable of modeling wave propagation in attenuating media with high accuracy. Using a sign reversal, we formulate a Q-compensated operator for reverse-time migration to correct for velocity dispersion and amplitude attenuation at the same time. Synthetic experiments show that the proposed method applied to viscoacoustic data produces subsurface images that are comparable in quality with the results obtained by acoustic RTM applied to acoustic data.

ACKNOWLEDGMENTS

We thank Associate Editor Joakim Blanch, Yu Zhang and one anonymous reviewer for their constructive comments. We thank the sponsors of the Texas Consortium for Computation Seismology (TCCS) for financial support. The first author was additionally supported by the Statoil Fellows Program at the University of Texas at Austin. The second author was supported by the Jackson School Distinguished Postdoctoral Fellowship at the University of Texas at Austin. We thank TACC (Texas Advanced Computing Center) for providing computational resources used in this study.

REFERENCES

Blanch, J. O., J. O. Robertsson, and W. W. Symes, 1995, Modeling of a constant q: methodology and algorithm for an efficient and optimally inexpensive viscoelastic technique: Geophysics, **60**, 176–184.

Blanch, J. O., and W. W. Symes, 1995, Efficient iterative viscoacoustic linearized inversion: 65th Ann. Internat. Mtg, Soc. of Expl. Geophys., 627–630.

Caputo, M., and F. Mainardi, 1971, A new dissipation model based on memory mechanism: Pure and Applied Geophysics, **91**, 134–147.

Carcione, J. M., 2007, Wave fields in real media: Theory and numerical simulation of wave propagation in anisotropic, anelastic, porous and electromagnetic media, 2nd ed.: Elsevier.

———, 2009, Theory and modeling of constant-Q P- and S-waves using fractional time derivatives: Geophysics, **74**, T1–11.

———, 2010, A generalization of the Fourier pseudospectral method: Geophysics, **75**, A53–A56.

Carcione, J. M., F. Cavallini, F. Mainardi, and A. Hanyga, 2002, Time-domain seismic modeling of constant-Q wave propagation using fractional derivatives: Pure and Applied Geophysics, **159**, 1719–1736.

Cavalca, M., R. Fletcher, and M. Riedel, 2013, Q-compensation in complex media - ray-based and wavefield extrapolation approaches: 83rd Ann. Internat. Mtg, Soc. of Expl. Geophys., 3831–3835.

Chen, W., and S. Holm, 2004, Fractional Laplacian time-space models for linear and nonlinear lossy media exhibiting arbitrary frequency power-law dependency: J. acoust. Soc. Am., **115**, 14241430.

Dutta, G., and G. T. Schuster, 2014, Attenuation compensation for least-squares reverse time migration using the viscoacoustic-wave equation: Geophysics, **79**, S251–S262.

Dvorkin, J. P., and G. Mavko, 2006, Modeling attenuation in reservoir and nonreservior rock: The Leading Edge, **25**, 194–197.

Fomel, S., L. Ying, and X. Song, 2013, Seismic wave extrapolation using lowrank symbol approximation: Geophysical Prospecting.

Kjartansson, E., 1979, Constant-Q wave propagation and attenuation: Journal of Geophysical Research, **84**, 4737–4748.

Lin, R., F. Liu, V. Anh, and I. Turner, 2009, Stability and convergence of a new explicit finite-difference approximation for the variable-order nonlinear fractional diffusion equation: Applied Mathematics and Computation, **212**, 435–445.

Liu, H. P., D. L. Anderson, and H. Kanamori, 1976, Velocity dispersion due to anelasticity: Implication for seismology and mantle composition: Geophysical Journal of the Royal Astronomical Society, **47**, 41–58.

Podlubny, I., 1999, Fractional Differential Equations: Academic Press.

Robertsson, J. O., J. O. Blanch, and W. W. Symes, 1994, Viscoacoustic finite-difference modeling: Geophysics, **59**, 1444–1456.

Sun, J., and S. Fomel, 2013, Low-rank one-step wave extrapolation: 83th Ann. Internat. Mtg., Soc. Expl. Geophys., 3905–3910.

Sun, J., S. Fomel, and J. Hu, 2014, One-step least-squares reverse-time migration using two-way wave extrapolation by non-stationary phase shift: 84th Ann. Internat. Mtg., Soc. Expl. Geophys., submitted.

Valenciano, A. A., and N. Chemingui, 2012, Viscoacoustic imaging: tomographic Q estimation and migration compensation: 82nd Ann. Internat. Mtg, Soc. of Expl. Geophys., 1–5.

Zhang, Y., P. Zhang, and H. Zhang, 2010, Compensating for viscoacoustic effects in reverse-time migration: 80th Ann. Internat. Mtg, Soc. of Expl. Geophys., 3160–3164.

Zhu, T., 2014, Time-reverse modeling of acoustic wave propagation in attenuating media: Geophysical Journal International, **197**, 483–494.

Zhu, T., J. M. Carcione, and J. M. Harris, 2013, Approximating constant-Q seismic propagation in the time domain: Geophysical Prospecting, **61**, 931–940.

Zhu, T., and J. M. Harris, 2014, Modeling acoustic wave propagation in heterogeneous attenuating media using decoupled fractional Laplacians: Geophysics, **79**, T105–T116.

Zhu, T., J. M. Harris, and B. Biondi, 2014, Q-compensated reverse-time migration: Geophysics, **79**, S77–S87.